

Highly-reduced Fine-structure splitting in InAs/InP quantum dots offering efficient on-demand 1.55 μm entangled photon emitter

Lixin He ^{*},¹ Ming Gong,¹ Chuan-Feng Li,¹ Guang-Can Guo,¹ and Alex Zunger²

¹Key Laboratory of Quantum Information, University of Science and Technology of China, Hefei, 230026, People's Republic of China
²National Renewable Energy Laboratory, Golden, Colorado, 80401, USA
(Dated: November 5, 2018)

To generate entangled photon pairs via quantum dots (QDs), the exciton fine structure splitting (FSS) must be comparable to the exciton homogeneous line width. Yet in the (In,Ga)As/GaAs QD, the intrinsic FSS is about a few tens μeV . To achieve photon entanglement, it is necessary to Cherry-pick a sample with extremely small FSS from a large number of samples, or to apply strong in-plane magnetic field. Using theoretical modeling of the fundamental causes of FSS in QDs, we predict that the intrinsic FSS of InAs/InP QDs is an order of magnitude smaller than that of InAs/GaAs dots, and better yet, their excitonic gap matches the 1.55 μm fiber optic wavelength, therefore offer efficient on-demand entangled photon emitters for long distance quantum communication.

PACS numbers: 78.67.-n, 73.21.La, 42.50.-p

Entangled photon pairs distinguished themselves from the classically correlated photons because of their non-locality[1, 2] and therefore play a crucial role in quantum information applications, including quantum teleportation[3], quantum cryptography[4] and distributed quantum computation[5], etc. Benson *et al.*[6] proposed that a biexciton cascade process in a self-assembled QD can be used to generate the “event-ready” entangled photon pairs, with orders of magnitude higher efficiency than the traditional parametric down conversion method [2, 3, 4]. This process is shown schematically in Fig. 1(a), in which a biexciton decays into two photons via two paths of different polarizations $|H\rangle$ and $|V\rangle$. If the two paths are indistinguishable, the final result is a polarization entangled photon pair state[6, 7]($|H_{xx}H_x\rangle + |V_{xx}V_x\rangle$)/ $\sqrt{2}$. However, early attempts[6] to generate the entangled photon pairs using the InAs/GaAs QDs were unsuccessful, because the $|H\rangle$ - and $|V\rangle$ -polarized photons have a small energy difference due to the asymmetric electron-hole exchange interaction in the QDs [see Fig. 1(b)]. The small energy splitting, known as the fine structure splitting (FSS), is typically about $-40 \sim +80 \mu\text{eV}$ in the InAs/GaAs QDs [8, 9, 10], which is much larger than the radiative linewidth ($\sim 1.0 \mu\text{eV}$) [7, 11]. Such a splitting provides therefore “which way” information about the photon decay path that can destroy the photon entanglement, leaving only classically correlated photon pairs [7, 11].

To achieve photon entanglement, the FSS must be reduced to a value comparable to the exciton homogeneous line width. Lack of detailed understanding of the factors controlling FSS in QDs has thus far impeded the design of small FSS values in quantum systems. It was, however,

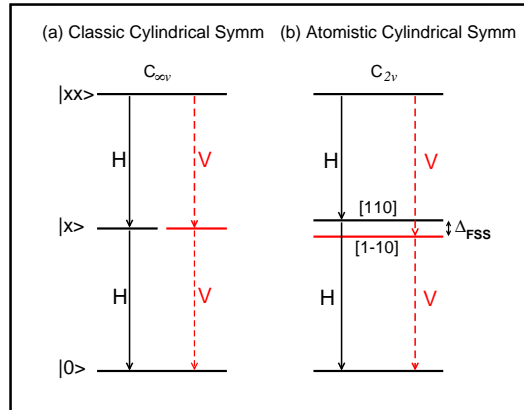


FIG. 1: (a) A schematic illustration of the biexciton cascade process to generate polarization entangled photons in a QD with classic cylindrical symmetry. H and V denote the polarization along the $[110]$ and $[1\bar{1}0]$ direction, respectively. (b) Due to the in-plane asymmetry, the H and V polarized photons have a small energy splitting Δ_{FSS} , which may destroy the polarization entanglement.

empirically discovered that the FSS in InAs/GaAs QDs can be significantly reduced or even reversed by various thermal annealing protocols [8, 10, 12]. Furthermore, in alloy dots of (In,Ga)As/GaAs, different random realizations of Ga and In distributions on the cation lattice lead a distribution of FSS values. Carefully screening of dots out of a large ensemble can then be used to [7] found those with small FSS. By applying such “Cherry Picking” techniques, entangled photon pairs have been recently achieved in the (In,Ga)As/GaAs QDs[7]. However, even after thermal annealing, the FSS is still about $\pm 10 \mu\text{eV}$, too large for generating entangled photon pairs[7]. The FSS can be further reduced by applying an in-plane magnetic field [7], which, however, significantly complicates

^{*}corresponding author: helx@ustc.edu.cn

the experimental setup. Other methods, e.g. applying in plane electric field, can also reduce the FSS[13]. However, the ensuing Stark effect greatly suppress the photoluminescence (PL) intensity[13]. Furthermore, after thermal annealing, the exciton wavelength is reduced to 880 ~ 950 nm, becoming uncomfortably close to the energy of the wetting layer emission, thus leading to unwanted strong background light[7, 14], and the wavelength is also too short for the optical fiber communications.

The reason for the early optimism about the use of QD for generating entangled photon pairs stems from the thought that FSS of an exciton will vanish [see Fig. 1(a)] in shape-symmetric dots (e.g, cylindrical, or lens-shaped or cone-shaped)[15]. However, the FSS of an exciton in a dot contains two terms: the previously largely ignored “intrinsic FSS” [15], which is nonzero even in a shaped-symmetric dot, and the “shape asymmetric FSS” due to deviation from geometric symmetry along $[110]$ and $[\bar{1}\bar{1}0]$ directions (e.g, lens-shaped with non-circular base)[12]. (Note that in this sense, the FSS is just like the spin-splitting effects, which are composed of the intrinsic Dresselhaus term, due to the bulk inversion asymmetry and the Rashba term, due to the geometrical asymmetry.) Whereas the contribution to the FSS of QD shape-asymmetric[12] can be reduced by carefully controlling the growth conditions, by annealing, or by cherry-picking the “right dots” out of an ensemble, the “intrinsic” FSS is still present even for an idea cylindrical dot, because semiconductor materials from which dots are commonly made have the well-known zinc-blende structure, and are thus not spatially isotropic. The zinc-blende structure has T_d symmetry, so even a cylindrically-shaped, i.e., lens or cone QD made of a zinc-blende semiconductor can only have a subgroup C_{2v} symmetry[16]. Since the interface between the dot material and the surrounding matrix material is not necessary a reflection plane, the (atomistic) potentials are different along the $[110]$ and $[\bar{1}\bar{1}0]$ directions[16]. This interfacial asymmetry leads to a natural, build-in “intrinsic FSS” [Fig. 1(b)] (even if atoms are unrelaxed, fixed to their ideal zinc-blende lattice sites). Such atomistic effects are commonly missed by continuum models (such as the effective mass approximation and the few-band k-p method), which only “see” the macroscopic shape symmetry, rather than atomistic details[17]. The intrinsic FSS is thus missed by these “low resolution” methods. However, recent atomistic calculations show that the intrinsic FSS is around several tens of μeV in the InAs/GaAs QDs [18].

Here we design a QD system with reduced FSS by using the microscopic understanding of the origins of the intrinsic FSS [18]. We recognize three factors here. First, atomic relaxation due to lattice size-mismatch between the dot and matrix materials (e.g, InAs and GaAs, respectively, have a 7% mismatch) enhances the magnitude of both intrinsic and shape asymmetry FSS[18]. Thus one could expect that the dot/matrix system with lower

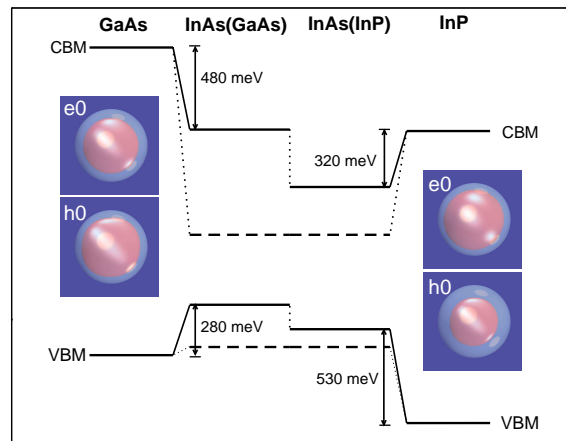


FIG. 2: Energy bandoffsets for the InAs/GaAs and InAs/InP QDs. The solid lines represent the strain modified bandoffsets, whereas the dashed line is the unstrained CBM and VBM for InAs. We show in the insert, the first electron (e_0) and hole (h_0) wavefunctions of the lens-shaped InAs/GaAs and InAs/InP QDs, with base= 25 nm, and height= 2.5 nm. The isosurface is chosen to enclose 95 % of the total density.

lattice mismatch should have smaller FSS. Second, a stronger confinement of the electron and hole in their respective potential wells will reduce the penetration of the respective wavefunctions into the matrix material, thus reducing their amplitude at the interface, where intrinsic asymmetry is present. Third, since the (atomistic) hole wavefunctions are more localized on the anion sites, having dot and matrix material with different anions (e.g, As vs P or N) will further reduces the amplitude of hole wavefunctions at the interface, thus reducing the intrinsic FSS.

Surprisingly, all three conditions can be met by retaining InAs as the dot material, but replacing the commonly used GaAs matrix material by InP. The latter material has a smaller lattice mismatch with InAs (3 % instead of 7 % for GaAs), and manifests a different anion (P) with respect to the As atom in GaAs. To examine the extent to which the InP matrix better confines the excitonic wavefunction inside the InAs dot, we compare in Fig. 2 the strain-modified potential in an InAs dot surrounded by GaAs or InP. Since the electron wavefunction (e_0 in the insert to Fig.2) is similar in both systems due to the light electron mass of InAs, the dimension of the excitonic wavefunction is mainly determined by the hole wavefunction. As shown in Fig. 2, the (strained) hole confining potential for InAs/InP is 530 meV, much larger than that for InAs/GaAs (46 meV). Consequently, the hole wavefunction of the InAs/InP system (h_0 in the insert to Fig. 2) is indeed much more localized in the dot interior than is the case in the InAs/GaAs dot[19]. The reduce wavefunction amplitude at the interface, where the $[110]$ vs $[\bar{1}\bar{1}0]$ asymmetry is maximal, will then re-

TABLE I: Geometries of the QDs used in the calculations. D is the base diameter of the lens-shaped and (truncated-)cone-shaped dots, whereas h is the height of the dots. S is defined as $R_{[110]} \cdot R_{[1\bar{1}0]}$, where $R_{[110]}$ and $R_{[1\bar{1}0]}$ are the diameters of the (elongated) QDs along $[110]$ and $[1\bar{1}0]$ direction, respectively.

	Shape	Size
L1	Lens	$D = 20$ nm, $h = 2.5$ to 5.5 nm
L2	Lens	$D = 25$ nm, $h = 2.5$ to 5.5 nm
L3	Lens	$h = 3$ nm, $D = 20$ to 25 nm
L4	Lens	$h = 4$ nm, $D = 20$ to 25 nm
L5	Lens	$h = 5$ nm, $D = 20$ to 25 nm
C1	Cone	$D = 20$ nm, $h = 2.5$ to 5.5 nm
C2	Cone	$D = 25$ nm, $h = 2.5$ to 5.5 nm
C3	Cone	$h = 3$ nm, $D = 20$ to 25 nm
C4	Cone	$h = 4$ nm, $D = 20$ to 25 nm
C5	Cone	$h = 5$ nm, $D = 20$ to 25 nm
E1	Elongated	$S = 20^2$ nm ² , $h = 4.5$ nm
E2	Elongated	$S = 25^2$ nm ² , $h = 4.5$ nm

duce the intrinsic FSS in InAs/InP.

To examine our design principles for reduced FSS at work, we carried out extensive calculations of the exciton energies and their FSS for 184 different dots in the InAs/InP and InAs/GaAs QDs. We have considered realistic sizes and geometries, including lens-shaped QDs (L1-L5), (truncated-)cone-shaped QDs (C1-C5) and elongated QDs (E1,E2) (see Table I). We use an atomistic pseudopotential approach to describe the single-particle physics[19, 20], and a configuration-interaction approach to describe the many-body interactions[21]. The atomic positions were relaxed to their minimum-strain position. Since the exciton and biexciton are nearly linearly polarized along the $[110]$ direction and the $[1\bar{1}0]$ direction, the FSS is defined as the energy splitting between the $[110]$ polarized exciton and $[1\bar{1}0]$ polarized exciton, i.e., $\Delta_{\text{FSS}} = E(X_{[110]}) - E(X_{[1\bar{1}0]})$.

Figure 3 shows the FSS in these two systems as a function of the excitonic energy[22]. The exciton energies of the (pure) InAs/GaAs QDs range from 0.95 - 1.12 eV, and the FSS scatters from - 18 μeV to 60 μeV , both are in a good agreement with experiments [8, 9, 10, 11, 12], which establishes credibility for the results of the InAs/InP dots. Figure 3 demonstrates that the intrinsic FSS of the InAs/InP QDs (-4 μeV to 6 μeV), is about an order of magnitude smaller than that of the InAs/GaAs QDs. This system can therefore be used as efficient entangled photon source. Furthermore, since the primary exciton wavelength of the InAs/InP QDs is around 1.55 μm telecom wavelength[19, 23, 24], they are very promising for the long distance quantum communication via optical fibers. The calculated FSS are consistent with recent experiments, in which extremely small exciton FSS were measured in the InAs/InP dots[23, 24]. However, it was not realized that the small FSS is an *intrinsic* property of the InAs/InP dots.

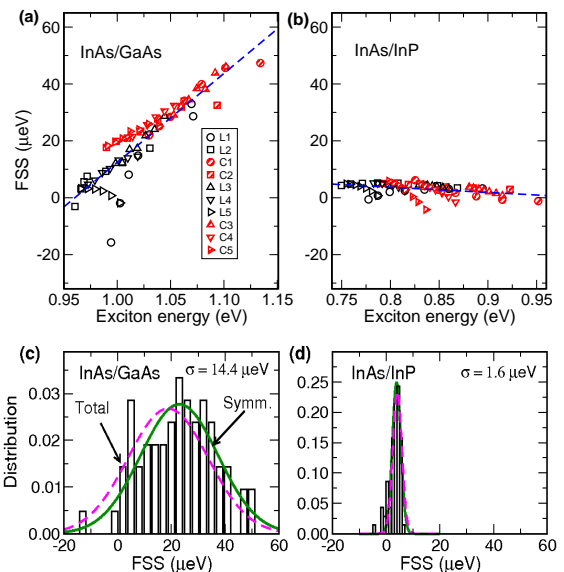


FIG. 3: The upper panel shows the FSS vs the exciton energy for (a) InAs/GaAs and (b) InP QDs. The lower panel shows the FSS distributions for (c) InAs/GaAs and (d) InP QDs. The solid lines are fitted by Gaussian functions for all shape-symmetric QDs, whereas the dashed lines represent the distributions of the FSS of total samples including also the asymmetric dots. σ is the standard deviation of the distribution.

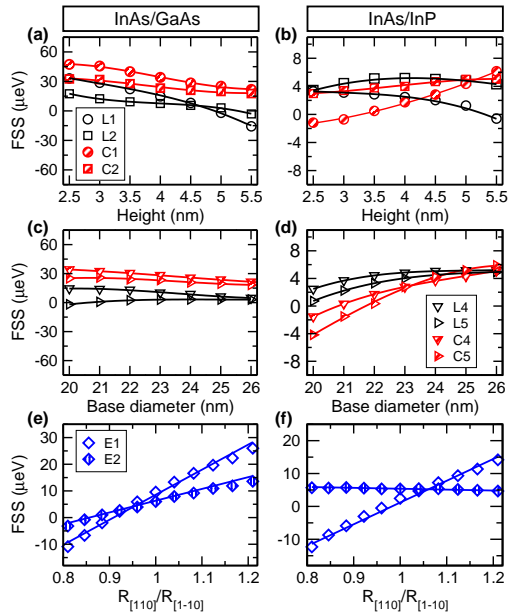


FIG. 4: Upper panel: The height dependence of the FSS for (a) InAs/GaAs and (b) InAs/InP QDs with different sizes and geometries (Lens and Cone). Middle panel: The base diameter dependence of the FSS for (c) InAs/GaAs and (d) InAs/InP QDs. Lower panel: The FSS as function of lateral aspect ratio of the elongated QDs in (e) InAs/GaAs and (f) InAs/InP QDs.

The FSS of the InAs/GaAs and InAs/InP QDs are compared in Fig. 4 for different dot geometries given in Table I. Figure I(a)-(d) show the results for shape-symmetric dots (circular-base), whereas parts (e)-(f) illustrate the effects of shape asymmetry (base with different radii lengths). We next discuss the trends with dot height, base size, and shape anisotropy:

Intrinsic FSS vs dot height: For the InAs/GaAs dots, we see the FSS decrease monotonically with increasing of the dot height. At about $h = 5$ nm, the FSS of the InAs/GaAs dot L1 is found to be zero. This is because in the tall InAs/GaAs QDs, the holes are localized at the interface of the dot due to the strain effect [25], which reduces the electron-hole wavefunction overlap, leading to small FSS. However, it is not a good way to reduce the FSS by increasing the dot height for the InAs/GaAs QDs, because the PL intensity is also reduced with the deduction of the FSS due to the reducing of electron-hole overlap. The height effect of the FSS is less dramatic for the InAs/InP dots, and all FSS are found to be extremely small (between $-4 \mu\text{eV}$ to $6 \mu\text{eV}$). A zero FSS is also found for the L1 InAs/InP dots at height ~ 5.5 nm. However, unlike in the InAs/GaAs dot, the holes are not localized on the interface in the InAs/InP QDs [19], therefore, it would not suffer the problem of PL intensity suppression as in the tall InAs/GaAs dots.

Intrinsic FSS as a function of dot base size: For flat InAs/GaAs QDs (L4, C4), the FSS decrease monotonically with increasing of the base size. However, for the tall InAs/GaAs dot(L5), as we increase the base size, the FSS increases, because the hole is less localized on the interface [25], which increases the electron-hole overlap, and thus the FSS. However, the FSS depends less on the base diameters than on the dot height for the InAs/GaAs dots. For InAs/InP dots, the FSS increase slightly as we increase the base size for all dot geometries. The FSS of the cone-shaped dots are similar to that of the lens-shaped dots.

Effect of Shape-asymmetry to FSS : Figure 4 (e) depicts the FSS of the InAs/GaAs QDs as functions of the lateral aspect ratio $R_{[110]}/R_{[1\bar{1}0]}$, whereas Fig. 4 (f) shows the results for the InAs/InP QDs, for two fixed dot volume and height. For InAs/GaAs QDs, we see that as we increase the asymmetric ratio the FSS increase dramatically from $-11 \mu\text{eV}$ to $26 \mu\text{eV}$. For the InAs/InP QDs, we found that for the smaller QDs, the FSS depends strongly on the shape asymmetry of QDs (from $-12 \mu\text{eV}$ to $14 \mu\text{eV}$), whereas for the larger dot, the FSS only weakly dependent on the shape-asymmetry.

Statistical distribution of FSS vs sizes and shapes : To further illustrate the differences of the FSS between the InAs/GaAs and the InAs/InP QDs, we plot the statistical distribution of FSS for the two types of dots in Fig. 3(c),(d) respectively. The solid lines represent the distributions of the intrinsic FSS of cylindrical QDs, fitted by Gaussian functions and the dashed line represent the

distributions of the FSS of total samples including also the asymmetric dots. As we see, including the asymmetric dots does not change much the FSS distribution. The mean value of the FSS of the InAs/GaAs dots is $23 \mu\text{eV}$, with standard deviation of 14.4 meV , whereas the average FSS of the InAs/InP dots is $3.5 \mu\text{eV}$ and standard deviation is only about $1.6 \mu\text{eV}$.

The FSS of the InAs/InP might still be too large to achieve perfect photon entanglement [7], but it can be further reduced by controlling the growth condition. For example, for the “small” InAs, InP lattice mismatch, one may try to grow a quantum disk, which has higher D_{2d} symmetry, thus (almost) zero FSS. Nevertheless, it is much easier to obtain the InAs/InP QDs with nearly zero FSS than the InAs/GaAs dots.

To conclude, we have shown that the *intrinsic* FSS of the InAs/InP dots are (statistically) about an order of magnitude smaller than that of the InAs/GaAs dots. The InAs/InP QDs have additional advantages because the emission photon wavelength is around $1.55 \mu\text{m}$, and is far away from the wetting layer background emissions. Combining these advantages, one can expect that the InAs/InP QDs can play a crucial role in the quantum information applications, as a new generation of “on-demanding” entangled photon source.

L.H. acknowledges the support from the Chinese National Fundamental Research Program 2006CB921900, the Innovation funds and “Hundreds of Talents” program from Chinese Academy of Sciences, and National Natural Science Foundation of China (Grant No. 10674124). A.Z. acknowledges support from USA DOE Office of Science, Basic Energy Science, Materials Sciences and Engineering, LAB-17 initiative, under Contract No. DE-AC36-99GO10337 to NREL.

-
- [1] A. Aspect, P. Grangier, and G. Roger, Phys. Rev. Lett. **49**, 91 (1982).
 - [2] Z. Y. Ou and L. Mandel, Phys. Rev. Lett. **61**, 50 (1988).
 - [3] T. Jennewein, G. Weihs, J.-W. Pan, and A. Zeilinger, Phys. Rev. Lett. **88**, 017903 (2001).
 - [4] N. Gisin, G. Ribordy, W. Tittel, and H. Zbinden, Rev. Mod. Phys. **74**, 145 (2002).
 - [5] J. I. Cirac, A. K. Ekert, S. F. Huelga, and C. Macchiavello, Phys. Rev. A **59**, 4249 (1999).
 - [6] O. Benson, C. Santori, M. Pelton, and Y. Yamamoto, Phys. Rev. Lett. **84**, 2513 (2000).
 - [7] R. M. Stevenson, R. J. Young, P. Atkinson, K. Cooper, D. A. Ritchie, and A. J. Shields, Nature **439**, 179 (2006).
 - [8] R. J. Young, R. M. Stevenson, A. J. Shields, P. Atkinson, K. Cooper, D. A. Ritchie, K. M. Groom, A. I. Tartakovskii, and M. S. Skolnick, Phys. Rev. B **72**, 113305 (2005).
 - [9] A. Högele, S. Seidl, M. Kroner, K. Karrai, R. J. Warburton, B. D. Gerardot, and P. M. Petroff, Phys. Rev. Lett. **93**, 217401 (2004).
 - [10] A. I. Tartakovskii, M. N. Makhonin, I. R. Sellers,

- J. Cahill, A. D. Andreev, D. M. Whittaker, J.-P. R. Wells, A. M. Fox, D. J. Mowbray, M. S. Skolnick, et al., Phys. Rev. B **70**, 193303 (2004).
- [11] N. Akopian, N. H. Lindner, E. Poem, Y. Berlatzky, J. Avron, D. Gershoni, B. D. Gerardot, and P. M. Petroff, Phys. Rev. Lett. **96**, 130501 (2006).
- [12] R. Seguin, A. Schliwa, S. Rodt, K. Pötschke, U. W. Pohl, and D. Bimberg, Phys. Rev. Lett. **95**, 257402 (2005).
- [13] B. D. Gerardot, S. Seidl, P. A. Dalgarno, R. J. Warburton, D. Granados, J. M. Garcia, K. Kowalik, O. Krebs, K. Karrai, A. Badolato, et al., Appl. Phys. Lett. **90**, 041101 (2007).
- [14] R. J. Young, R. M. Stevenson, P. Atkinson, K. Cooper, D. A. Ritchie, and A. J. Shields, New Journal of Physics **6**, 29 (2006).
- [15] M. Bayer, A. Kuther, A. Forchel, A. Gorbunov, V. B. Timofeev, F. Schäfer, J. P. Reithmaier, T. L. Reinecke, and S. N. Walck, Phys. Rev. Lett. **82**, 1748 (1999).
- [16] G. Bester and A. Zunger, Phys. Rev. B **71**, 045318 (2005).
- [17] A. Zunger, phys stat. sol (b) **224**, 727 (2001).
- [18] G. Bester, S. Nair, and A. Zunger, Phys. Rev. B **67**, 161306(R) (2003).
- [19] M. Gong, K. Duan, C. Li, R. Magri, G. A. Narvaez, and L. He, Phys. Rev. B **77**, 045326 (2008).
- [20] A. J. Williamson, L.-W. Wang, and A. Zunger, Phys. Rev. B **62**, 12963 (2000).
- [21] A. Franceschetti, H. Fu, L.-W. Wang, and A. Zunger, Phys. Rev. B **60**, 1819 (1999).
- [22] In present work, we show the *intrinsic* FSS for selected geometries, which should not be directly compared to the trend of the FSS vs exciton energy for a particular thermal annealing process, (e.g Ref. 8), because the structure and composition of the QDs change dramatically during the thermal annealing.
- [23] N. I. Cade, H. Gotoh, H. Kamada, H. Nakano, S. Ananthanasarn, and R. Nötzel, Appl. Phys. Lett. **89**, 181113 (2006).
- [24] D. Kim, J. Lefebvre, J. Mckee, S. Studenikin, R. L. Williams, A. Sachrajda, P. Zawadzki, P. Hawrylak, W. Sheng, G. C. Aers, et al., Appl. Phys. Lett. **87**, 212105 (2005).
- [25] L. He, G. Bester, and A. Zunger, Phys. Rev. B **70**, 235316 (2004).